Large, Tunable, and Reversible pH Changes by Merocyanine Photoacids

Citation for the original published paper (version of record):
Wimberger, L., Prasad, S., Peeks, M. et al (2021). Large, Tunable, and Reversible pH Changes by Merocyanine Photoacids. Journal of the American Chemical Society, 143(49): 20758-20768. http://dx.doi.org/10.1021/jacs.1c08810

JACS
JOURNAL OF THE AMERICAN CHEMICAL SOCIETY
pubs.acs.org/JACS
Article

Large, Tunable, and Reversible pH Changes by Merocyanine Photoacids

Laura Wimberger, Shyamal K. K. Prasad, Martin D. Peeks, Joakim Andréasson, Timothy W. Schmidt, and Jonathon E. Beves*

Cite This: J. Am. Chem. Soc. 2021, 143, 20758−20768
Read Online
ACCESS | Metrics & More | Article Recommendations | Supporting Information

ABSTRACT: Molecular photoswitches capable of generating precise pH changes will allow pH-dependent processes to be controlled remotely and noninvasively with light. We introduce a series of new merocyanine photoswitches, which deliver reversible bulk pH changes up to 3.2 pH units (pH 6.5 to pH 3.3) upon irradiation with 450 nm light, displaying tunable and predictable timescales for thermal recovery. We present models to show that the key parameters for optimizing the bulk pH changes are measurable: the solubility of the photoswitch, the acidity of the merocyanine form, the thermal equilibrium position between the spiropyran and the merocyanine isomers, and the increased acidity under visible light irradiation. Using ultrafast transient absorption spectroscopy, we determined the quantum yields for the ring-closing reaction and found that the lifetimes of the transient *cis*-merocyanine isomers ranged from 30 to 550 ns. Quantum yields did not appear to be a limitation for bulk pH switching. The models we present use experimentally determined parameters and are, in principle, able to predict the change in pH obtained for any related merocyanine photoacid.

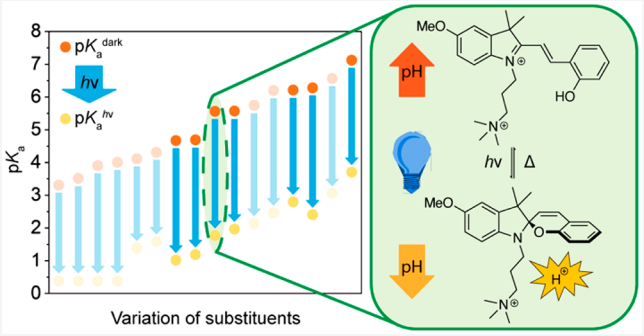

INTRODUCTION

Controlling pH environments is critical for many important chemical processes, including the biological operating ranges of enzymes and using proton gradients for energy storage. Tools for reversible pH control are highly sought after for mimicking biological systems and to control chemical processes like catalysis,[1] assembly/disassembly,[2] for generating out-of-equilibrium states,[3] or for controlling molecular machines.[4] It has long been recognized[5] that using light to reversibly control pH has advantages of being noninvasive and allows precise control in both time and space. One way to use light to control pH is with molecular photoacids. Photoacids are molecules whose excited states are substantially more acidic than the ground state. For example, 8-hydroxypyrene-1,3,6-trisulfonic acid (HPTS) exhibits a very large change in pK_a from the ground state (pK_a = 7.3) to the excited state (pK_a = 1.4).[6,7] The short lifetimes of the excited states, for example, 6 ns for HPTS,[7] prevent the buildup of significant proton concentration, and the resulting pH changes are limited, although some impressive applications have been reported.[8] Molecules that can be isomerized by visible light to long-lived metastable ground states are more suitable for controlling many protonation/deprotonation events.[9] Photoacids based on the spiropyran/merocyanine photoswitch[10] are generally the most versatile and widely used in part due to the large difference in effective pK_a between the spiropyran (SP) and merocyanine (MC(H)) forms (Figure 1).

The first merocyanine commonly used as a reversible photoacid was ethylene alcohol-functionalized merocyanine **1**.[11] This photoswitch was used in organic solvents for controlling self-assembly,[12] luminescence,[13] and optical signaling.[14] However, the relatively slow thermal recovery time (several days),[11b] relatively low pK_a, poor solubility of the spiropyran form in water,[15] and susceptibility of the merocyanine form to hydrolysis limited more widespread applications.

Liao[16] introduced a sulfonate group at the end of an alkyl chain attached to the indolinium nitrogen (position R^2, Figure 1) to prepare water-soluble merocyanine **2a**.[17] This photoacid allowed bulk pH switching by ∼2 pH units (pH 5.5 to 3.5), with a thermal half-life of 70 s for the pH recovery in the dark. The large jump in pH and the relatively rapid thermal recovery allowed this photoswitch to be applied in diverse contexts. Examples are the controlled self-assembly of discrete[18] or extended structures,[18d,19] including DNA structures[3c,20] or nanoparticles,[21] and influencing the properties of nano-

Received: August 20, 2021
Published: November 30, 2021

https://doi.org/10.1021/jacs.1c08810
J. Am. Chem. Soc. 2021, 143, 20758−20768

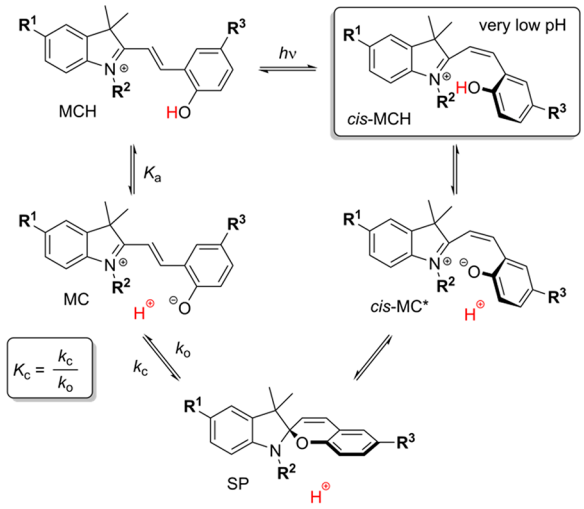

	R1	R2	R3	Ref.
1	H	$(CH_2)_2OH$	NO_2	Ref. 11
2a	H	$(CH_2)_3SO_3^-$	H	Ref. 16a / Ref. 31 / This work
2b	H	$(CH_2)_3SO_3^-$	*t*Bu	This work
2c	OMe	$(CH_2)_3SO_3^-$	*t*Bu	This work
2d	H	$(CH_2)_3SO_3^-$	NO_2	This work / Ref. 38
3a	H	$(CH_2)_3NMe_3^+$	H	This work
3b	H	$(CH_2)_3NMe_3^+$	*t*Bu	This work
3c	OMe	$(CH_2)_3NMe_3^+$	*t*Bu	This work
3d	OMe	$(CH_2)_3NMe_3^+$	H	This work

Figure 1. Merocyanine photoacid (photo)thermal equilibrium of **2a**–**3d** prepared in this study. The *cis*-MC* isomer is a transient species.

reactors,[22] soft materials,[23] gels,[24] and dyes.[25] Other applications include the control of polymerizations,[26] hydrazone molecular switches,[27] enhancing photophosphorylation by chloroplasts,[28] and operating molecular machines.[29] Building on earlier investigations,[30] Pezzato and co-workers recently reported a detailed study that significantly progressed the understanding of the thermodynamic and kinetic parameters of photoacid **2a**.[31] Using optimized conditions, the authors also demonstrated a 2.5 unit pH jump (from ∼6.1 to ∼3.6 pH)[31] and very recently improved it to approximately 3 pH units (from ∼7 to ∼4 pH).[32]

Despite these advances, designing merocyanine photoacids to deliver specific pH changes remains a significant challenge as the observed pH jump depends on several chemical/photophysical properties for which the structure–property relationships are not fully understood. Here, we introduce merocyanines **2b**–**3d**, investigate their photoacidic properties, and identify the key parameters that control the bulk pH change by merocyanines, providing clear guidelines for their ideal application and highlighting their limitations.

In the dark, merocyanine photoacids exist predominantly in three forms:[10] protonated merocyanine (MCH), deprotonated merocyanine (MC), and spiropyran (SP); see Figure 1. The MC undergoes thermal ring-closing (rate constant k_c) to form SP, which can ring-open (rate constant k_o) in the reverse reaction to give an equilibrium constant K_c, as in eq 1.

$$K_c = \frac{[SP]}{[MC]} = \frac{k_c}{k_o} \tag{1}$$

The thermal equilibrium between MC and SP (K_c) is inherently linked to the protonation equilibrium (K_a) between MCH and MC, as in eq 2.

$$K_a = \frac{[MC][H^+]}{[MCH]} \tag{2}$$

At pH values where MC is preferentially protonated, MCH is thermodynamically stable, and the equilibrium can be shifted entirely to the MCH form at sufficiently low pH.[33] Under visible light irradiation, the MCH undergoes *trans* to *cis* isomerization[34] to form *cis*-MCH, which is reportedly more acidic than MCH.[31,35] Thus, *cis*-MCH can only be observed at very low pH.[31,36] The deprotonation to *cis*-MC leads to fast ring-closure to the SP form,[35] resulting in increased proton concentrations under irradiation and as such acting as a photoacid.

RESULTS AND DISCUSSION

We synthesized a small library of merocyanines **2a**–**d**, **3a**–**d** in two or three steps (for details on the preparation and characterization, see Supporting Information S2–S4) and used the reported[31] **2a** as a reference compound. Substituents were introduced in three different positions (Figure 1; R^1, R^2, and R^3) to study their effects on the proton dissociation behavior. An increase in pK_a values is desirable as this would allow applications near neutral pH values. We opted for unsubstituted phenolic moieties or substitution with a weakly electron-donating group (R^3 = ^{t}Bu). This is to prevent a decrease of the pK_a value, which occurs when the molecule is substituted with electron-withdrawing groups that can stabilize the negative charge on the phenolate oxygen.[10a,16a,33a] Introducing a methoxy group on the indolinium ring (R^1 = OMe) has been reported[37] to increase the pK_a value, so we included examples in our study to explore this effect. Very recently, it was also shown that the introduction of a methoxy group in this position improves the hydrolytic stability.[32] We studied the effects of the alkyl side chain (R^2) by comparing a negatively charged sulfonate group and a positively charged trimethylammonium group.[33a] We used compound **2d**[38] to confirm the differences between merocyanines containing an electron-donating versus an electron-withdrawing group (R^3) in addition to comparison with the literature. To determine the change in acidity upon light irradiation of our merocyanines, we applied a recently reported methodology by Pezzato and co-workers.[31] A series of equilibrated UV–visible absorption spectra were collected at different pH values in the dark and under visible light irradiation. Representative data for photoacid **3d** are shown in Figure 2. The data were fit to a sigmoidal function to determine the acidity in the dark, pK_a^{dark}, and under irradiation, p$K_a^{h\nu}$, defined as[31] (see Supporting Information S6.5 for details):

$$K_a^{dark} = \frac{[H^+]([MC] + [SP])}{[MCH]} = K_a(1 + K_c) \tag{3}$$

$$K_a^{h\nu} = \frac{[H^+][SP]}{[cis\text{-}MCH]} \tag{4}$$

The photoacidity Π is calculated[31] as the difference between pK_a^{dark} and p$K_a^{h\nu}$. The values obtained for all compounds are shown in Table 1. Photoacid **2a** served as a reference compound, and our obtained values are in good agreement with the literature.[31] The experimentally observed pK_a^{dark} value is not equivalent to the pK_a value of the MCH form, as previously noted.[31] The pK_a^{dark} value considers the K_a and the K_c equilibria because the deprotonation of MCH to MC is linked to the ring-closure to form SP. This implies that pK_a^{dark} approaches pK_a of MCH when the equilibrium shifts sufficiently toward MC (i.e., $K_c \approx 0$, $[SP] \approx 0$) or if the rate of ring-closure is very slow (i.e., low k_c, as for **2d**). In all other cases, the shift in the equilibrium toward the SP form (i.e., $K_c\uparrow$) leads to a decrease in the pK_a^{dark}

https://doi.org/10.1021/jacs.1c08810
J. Am. Chem. Soc. 2021, 143, 20758–20768

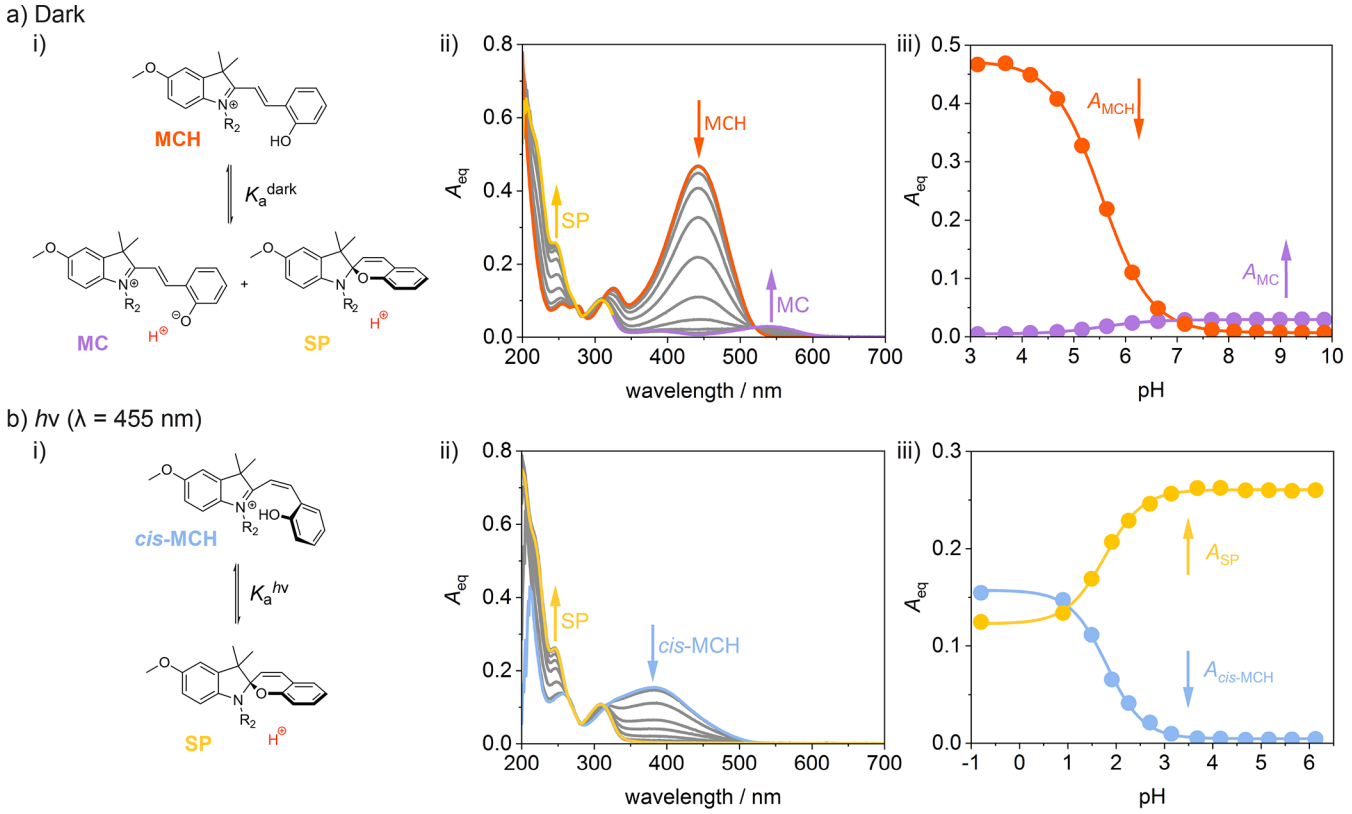

Figure 2. (a) pK_a^{dark} determination. (i) The K_a^{dark} equilibrium between photoacid **3d**-MCH and the deprotonated forms **3d**-MC and **3d**-SP. (ii) Equilibrated UV−vis absorbance spectra of photoacid **3d** in the dark over a range of pH values (orange, pH = 3.1; yellow/purple, pH = 9.9). (iii) The change in absorbance maxima at equilibrium characteristic for the individual species (orange, λ_{MCH} = 442 nm; purple, λ_{MC} = 538 nm) over the pH range with corresponding fits to eq S1 (Supporting Information S6.4) to determine pK_a^{dark} (inflection point). Experimental conditions: [**3d**] = 16.3 μM, [phosphate buffer] = 20 mM, pH 2.7−9.9, T = 25 °C. (b) $pK_a^{h\nu}$ determination. (i) The $K_a^{h\nu}$ equilibrium between photoacid **3d**-*cis*-MCH and the deprotonated form **3d**-SP. (ii) Equilibrated UV−vis absorbance spectra of photoacid **3d** under blue light irradiation (λ = 455 nm) at different pH values (blue, pH = −0.8; yellow, pH = 6.1). (iii) The change in absorbance maxima characteristic for the individual species (yellow, λ_{SP} = 246 nm; blue, $\lambda_{cis\text{-}MCH}$ = 383 nm) over the pH range with corresponding fits to eq S1 (Supporting Information S6.4) to determine $pK_a^{h\nu}$. Experimental conditions: $h\nu$ (λ = 455 nm), [**3d**] = 16.3 μM, [phosphate buffer] = 20 mM, pH −1.1−6.1, T = 25 °C.

value with respect to the pK_a value of MCH (i.e., $pK_a^{dark} \leq pK_a$). As far as we are aware, many previously reported "pK_a" values of merocyanines are pK_a^{dark} values, unless the above criteria is met (i.e., very low K_c or very low k_c).

The $pK_a^{h\nu}$ value determined under irradiation can be viewed as the pK_a value of the *cis*-MCH form because the equilibrium between *cis*-MC and SP is shifted entirely to SP when irradiated. The *cis*-MC form is short-lived and can only be detected by transient absorption spectroscopy,[35,39] whereas *cis*-MCH is stable at low pH values (determined by $pK_a^{h\nu}$).[36,40] In earlier studies, the *cis*-MCH was assigned as the protonated spiropyran (SPH).[10a,33a,41a,b] More recent work has shown that the assignment as *cis*-MCH is most appropriate.[36] From a practical perspective, *cis*-MCH behaves mechanistically as SPH due to an apparent barrierless transition from SP to *cis*-MCH at low pH.[36]

The pK_a^{dark} and $pK_a^{h\nu}$ values obtained for our library of compounds cover a range between 4.52−7.11 for pK_a^{dark} and 1.03−3.72 for $pK_a^{h\nu}$. The introduction of a methoxy group onto the indolinium ring (R^1, Figure 1) caused an increase of ca. one unit for both for pK_a^{dark} and for $pK_a^{h\nu}$ in all compounds (i.e., **2b** *vs* **2c**; **3a** *vs* **3d**; **3b** *vs* **3c**). By contrast, introducing a *tert*-butyl group (R^3, Figure 1) had a negligible effect on the pK_a^{dark} and $pK_a^{h\nu}$ values (i.e., **2a** *vs* **2b**; **3a** *vs* **3b**; **3d** *vs* **3c**). The alkylsulfonate-substituted (R^2, Figure 1) compounds **2a**−**2c** have pK_a^{dark} and $pK_a^{h\nu}$ values ∼1.5−1.7 units higher than those of alkylammonium-substituted photoacids **3a**−**3d**. By removing electron-withdrawing groups (R^3) and adding a methoxy group to the indolinium moiety (R^1), we could significantly increase the pK_a^{dark} and $pK_a^{h\nu}$ values of the alkylammonium compounds. For example, the pK_a^{dark} and $pK_a^{h\nu}$ values for **3d** are up to 1.3 units higher than those reported for known compounds **6**−**11**[33a] (3.3−4.3 for pK_a^{dark} and 0.4−1.6 for $pK_a^{h\nu}$). An overview of pK_a^{dark} and $pK_a^{h\nu}$ values of this study (Table 1) as compared to the reported values is shown in Figure 3. Interestingly, modifying the electronic properties by changing the substitution patterns appears to similarly influence pK_a^{dark} and $pK_a^{h\nu}$, resulting in a relatively constant photoacidity parameter Π (3.4−3.9) for our compounds. The known photoacid **2a** retained the highest Π value of 3.9 units. As we explain later, Π is not the main limiting factor for generating bulk pH changes in aqueous solutions, as other properties like the solubility of the compounds play a substantial role.

To better understand the effects of the substitution pattern on the pK_a^{dark} values, we determined the K_c values for photoacids **2a**−**c**, **3a**−**d** followed by calculation of the respective pK_a values. The rate constants of the ring-opening/-closing reaction (k_o/k_c) of the photoacids were determined by the addition of a sample of each photoacid to buffered solutions and monitoring the equilibration process by UV−vis absorbance spectroscopy. We fit the intensity of the MC (or MCH) visible absorption over

https://doi.org/10.1021/jacs.1c08810
J. Am. Chem. Soc. 2021, 143, 20758−20768

Table 1. Critical Parameters of Merocyanine Photoacids 1, 2a–d, and 3a–d

	pK_a^{dark}[a]	$pK_a^{h\nu}$[a]	Π[b]	$k_o/10^{-2}$ s^{-1}	$k_c/10^{-2}$ s^{-1}	K_c[c]	pK_a[d]	$\Phi_{MCH\rightarrow SP}$[e]
1[f]	4.52[f]			7.6×10^{-3}[f]			4.52[f]	
2a	6.27 ± 0.02	2.42 ± 0.04	3.85 ± 0.08	0.54 ± 0.1[h]	2.8 ± 0.5[h]	5.2 ± 1	7.07 ± 0.10	0.11
	(6.19 ± 0.06)[g]	(2.47 ± 0.04)[g]	(3.7 ± 0.1)[g]	(0.45)[g]	(3.9)[g]	(8.6 ± 4.9)[g]	(7.20 ± 0.03)[g]	(0.37 ± 0.04)[g,i]
2b	6.20 ± n.a.	2.81 ± 0.04	3.39 ± 0.04	1.7 ± 0.3[h]	15 ± 3[h]	8.6 ± 2	7.18 ± 0.11	0.04
2c	7.11 ± 0.03	3.72 ± 0.01	3.38 ± 0.03	1.9 ± 0.3[h]	2.3 ± 0.5[h]	1.2 ± 0.3	7.46 ± 0.07	0.16
2d[j]	4.66 ± 0.04[k]	1.88 ± 0.03	2.78 ± 0.05	0.0038[l]	0.0021[m]	0.55[n]	4.85 ± 0.04[o]	
							(4.72)[p]	
3a	4.66 ± 0.04	1.03 ± 0.08	3.63 ± 0.09	0.18[l]	22 ± 4[h]	123 ± 23	6.76 ± 0.09	0.06
3b	4.68 ± 0.08	1.20 ± 0.02	3.48 ± 0.08	0.57[l]	104 ± 22[h]	183 ± 40	6.95 ± 0.12	0.03
3c	5.56 ± 0.01	1.98 ± 0.01	3.58 ± 0.01	0.62[l]	25 ± 6[h]	41 ± 10	7.18 ± 0.10	0.11
3d	5.55 ± n.a.	1.78 ± 0.03	3.76 ± 0.03	0.17[l]	4.4 ± 0.9[h]	26 ± 5	6.97 ± 0.08	0.03

[a] pK_a^{dark}: Experimentally observed value for the proton dissociation of the MCH form, $pK_a^{dark} \neq pK_a$. $pK_a^{h\nu}$: Experimentally observed value for the proton dissociation of the photoacids under blue light irradiation (λ = 455 nm), equivalent to the pK_a of *cis*-MCH. pK_a^{dark} and $pK_a^{h\nu}$ were determined from the fit to eq S1 (Supporting Information S6.4) and reported as the average of two fits; error from standard deviation (n.a. = error negligible). [b] Photoacidity parameter: $\Pi = pK_a^{dark} - pK_a^{h\nu}$; uncertainty from error propagation. [c] Thermal equilibrium constant describing MC ⇌ SP as defined in Figure 1, calculated from eq 1 (Supporting Information S6.6); uncertainty from error propagation. [d] Calculated from eq 6 with pK_a^{dark} experimentally determined from fit to eq S1 (Supporting Information S6.4) and K_c from eq 1 (Supporting Information S6.6). [e] Quantum yields for the SP formation from MCH determined by transient absorption (Supporting Information S7). [f] Reported for MCH in water; assuming SP has negligible solubility, we determine that this value would also be the pK_a; see ref 15. [g] k_c, k_o, and K_c values from Tables 1 and S1 in ref 31. [h] k averaged over three temperatures (T = 25 ± 1.5 °C) extracted from the linear fit in the Eyring plot; errors calculated by standard deviation (details in Supporting Information S6.6). [i] From ref 42. [j] Significant hydrolysis was observed at pH values where the merocyanine form is deprotonated. The rate of hydrolysis k_{hydr} was determined as 1.6×10^{-5} s^{-1}; for details, see Supporting Information S6.6. [k] Calculated from $pK_a^{dark} = -\log(K_a(1 + K_c))$ with K_a determined from the fit to eq S1. [l] Error from single exponential fit is negligible; temperature dependence was not determined. [m] Determined from the fit to eq S15. [n] Temperature-dependent error was not determined; error from fit is negligible. [o] Because of slow thermal equilibration, the experimentally observed $pK_a \neq pK_a^{dark}$, determined from the fit to eq S1 (Supporting Information S6.4). [p] From ref 37.

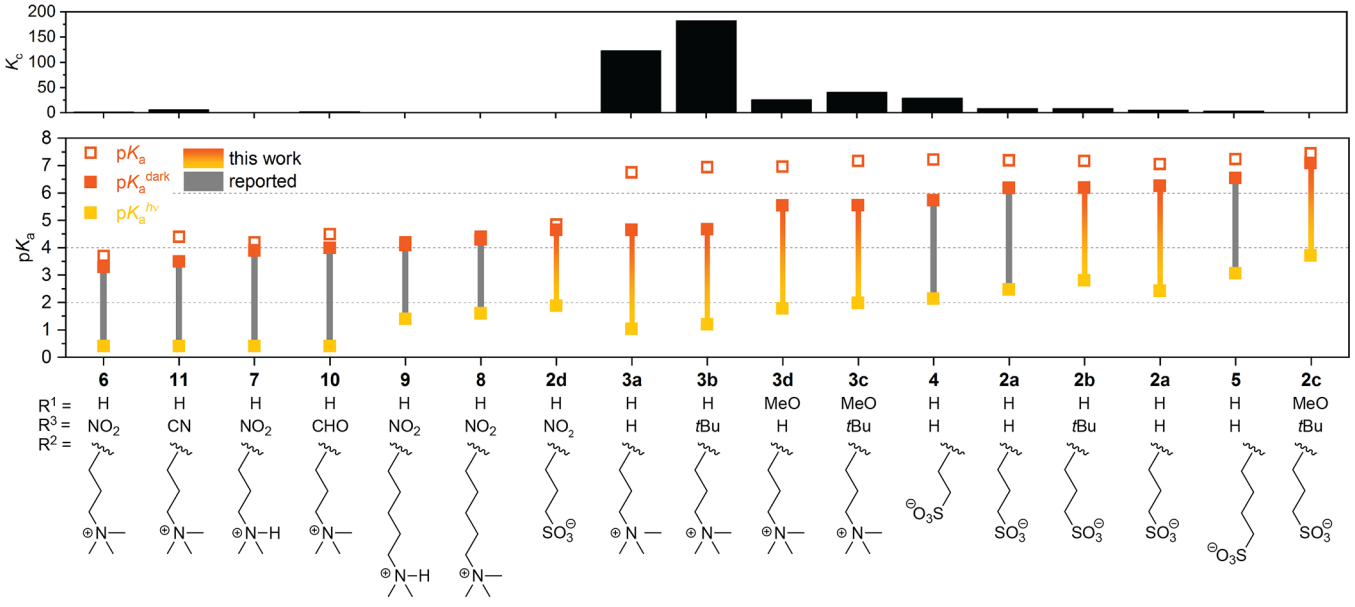

Figure 3. Overview of the photoacidity parameters of our study (orange-yellow bars) as compared to the literature (Supporting Information S11.5) (gray bars),[31,33a] $pK_a^{h\nu}$ (yellow), pK_a^{dark} (orange), and pK_a (orange box) values of photoacids with their corresponding K_c values shown above.

time (A_t) to the exponential function given in eq 5 to obtain the observed thermal equilibration rate constant, k_{obs}, at different pH values:

$$A_t = A_{eq} + (A_0 - A_{eq})\, e^{-k_{obs}t} \quad (5)$$

where A_{eq} is the absorption at equilibrium and A_0 is the absorption at the start of the measurement.

The varying degree of protonation coincided with a change in k_{obs} over the pH range (Figure 6a; see Supporting Information S6.6 for other compounds). At low pH (pH ≪ pK_a), k_{obs} is equal to k_o as the ring-closing reaction is impeded by protonation of MC, which gives the thermodynamically stable MCH form.[31,33a] The rate constants for the ring-closing reaction (k_c) of photoacids **2a–c** were determined following a reported procedure[31] by monitoring the equilibration process at high pH with UV–vis absorbance spectroscopy. At high pH (≫pK_a, [MCH] ≈ 0), the observed rate constant is equal to the sum of the ring-closing and ring-opening reactions ($k_{obs} = k_o + k_c$), as expected for a reversible first-order process. Photoacids **3a–d** have significantly faster rates of ring-closing, which prevented application of this method. Instead, we observed the equilibration process by perturbing the equilibrium by UV-

https://doi.org/10.1021/jacs.1c08810
J. Am. Chem. Soc. 2021, 143, 20758–20768

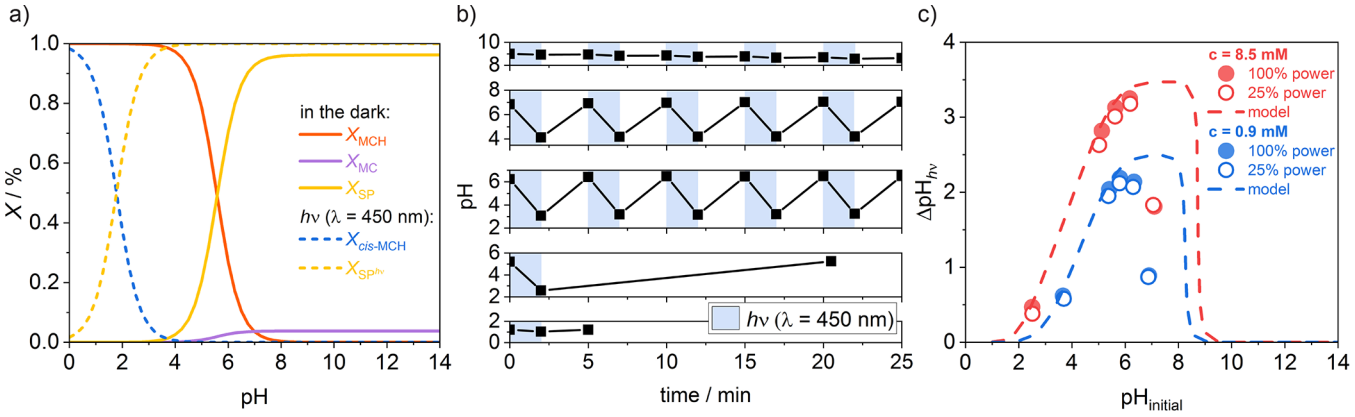

Figure 4. Photoacid **3d**. (a) Calculated mole fractions in the dark and under irradiation over the pH range (see Supporting Information S6.7). (b) Visible light-induced (λ = 450 nm, indicated by blue boxes) pH switching of concentrated aqueous solutions of photoacid **3d** at different initial pH values. (c) Experimental pH changes under irradiation ($\Delta pH_{h\nu}$) achieved at the respective initial pH values in comparison to the model predicting pH changes under irradiation.

irradiation (265 nm) at high pH, using a custom-made setup to give a higher time resolution (details in Supporting Information S6.3). The K_c values were then calculated using eq 1. Variable-temperature studies of the equilibration process also allowed us to define a temperature-based error of K_c (see Supporting Information S6.6).

The K_c values of the alkylsulfonate compounds **2a–d** lay in the range of 0.6–9, and the value for photoacid **2a** agrees with the reported values (5.2 ± 1 vs 8.6 ± 4.9, ref 31). The K_c values of the alkylammonium compounds **3a–d** are significantly higher, ranging from ∼30 to ∼180, meaning the SP form is largely preferred over the MC form.

The thermodynamic preference of the SP form is related to a decrease in the stability of the positive charge on the indolinium nitrogen in the MC/MCH forms. For alkylammonium compounds **3a–d**, the positive charge of the side chain appears to destabilize the positive charge of the indolinium nitrogen, leading to an increased relative stability of the SP form (high K_c). By comparison, the negatively charged alkylsulfonate side chain in **2a–d** has a more stabilizing effect on the MC form (lower K_c). The distance between the charge on the side chain and that on the indolinium nitrogen has been previously reported to have an influence on the relative stability of the MC form (e.g., compound **2a** vs **4** and **5**; **6** vs **8**; **7** vs **9**; see Figure 3 for structures).[31,33a] The positively charged alkyl ammonium side chain also results in lower pK_a values than those of the sulfonate derivatives. For example, the pK_a^{dark} of **3a** is 1.6 units lower than that of **2a**; the pK_a^{dark} of **6** is 1.2 units lower than that of **2d**.

Introducing a methoxy group on the indolinium ring (R^1) appears to have a stabilizing effect on the positively charged nitrogen, leading to a decrease in K_c. By contrast, substitution on the phenolic moiety (R^3) has a minimal effect on K_c. For all compounds, higher K_c values led to a higher acidity of the system (i.e., $pK_a^{dark}\downarrow$ and $pK_a^{h\nu}\downarrow$).

The pK_a values of MCH were calculated from the pK_a^{dark} and K_c values by modification of eq 3 to give:

$$pK_a = pK_a^{dark} + \log(1 + K_c) \quad (6)$$

The obtained pK_a value of 7.07 ± 0.10 for **2a** is in good agreement with the literature reports[31] (7.20 ± 0.03), and photoacids **2b–c** have similar values in the range of 7.18–7.46. The pK_a values of **3a–d** are also quite similar (6.76–7.18). Reported merocyanine photoacids[33a] **6–11** as well as **2d** have significantly lower pK_a values (3.7–4.9) as they are substituted with electron-withdrawing groups on the phenolic ring (Figure 3, R^3 = NO_2, CN, CHO), which stabilize the negative charge on the phenolate oxygen.

Spiropyran derivatives with an electron-withdrawing nitro group *para* to the phenol are known to be slow to ring open,[38] and the MC forms are susceptible to hydrolysis.[33a] We confirmed these properties by preparing known[38] alkylsulfonate derivative **2d** (R^3 = NO_2) and find the rates of ring-opening and hydrolysis to be comparable, but slow ($k_h = 10^{-5}$ s^{-1}; for details of the kinetic analysis, see Supporting Information S6.6). The pK_a value (pK_a = 4.85) we determined was also in agreement with the reported value (pK_a = 4.72).[37] The analogous compound with an alkyl ammonium side chain, compound **6**, is also known to be slow to ring-open and to be similarly susceptible to hydrolysis,[33a,43] making nitro-functionalized merocyanines unsuitable for most photoacid applications.

Comparison of our K_c and pK_a values and previously reported values (Figure 3, Supporting Information S11.5)[31,33a] suggests that the pK_a value can be tuned by introducing electron-donating ($pK_a\uparrow$) or electron-withdrawing groups ($pK_a\downarrow$) as might be expected. The experimentally observed and "effective" pK_a^{dark} value can be increased by stabilizing the positive charge ($K_c\downarrow$) on the indolinium nitrogen of the MC(H) form. The maximum achievable pK_a^{dark} is the pK_a value where $K_c \ll 1$. For optimized pH switching, a small K_c and a high pK_a value are required to result in a high pK_a^{dark} value.

We studied the achievable pH changes caused by the photoacids over a pH range. This required considering the following key parameters: (1) the logarithmic scale of pH, as higher pH values require a smaller concentration of protons to induce a pH change; (2) the autoionization of water (K_w) at high pH values; (3) the solubility of the photoacid, as higher [MCH] will result in a higher concentration of released protons upon irradiation; (4) pK_a^{dark} that defines the concentration of MCH present at the respective pH values; (5) $pK_a^{h\nu}$, [*cis*-MCH] under irradiation that defines a lower limit of proton dissociation; and (6) the extent of photoswitching, as full conversion of MCH to SP under irradiation generates the maximum concentration of released protons.

To evaluate the pH switching, we first calculated the mole fractions of the individual species (MCH/MC/SP) over the pH range in the dark using pK_a and K_c. The mole fractions under

https://doi.org/10.1021/jacs.1c08810
J. Am. Chem. Soc. 2021, 143, 20758–20768

irradiation (*cis*-MCH/SP) were calculated using $pK_a^{h\nu}$ assuming a complete bleach of the MCH form. The distribution of the individual species over the pH range is shown for photoacid **3d** in Figure 4a (see Supporting Information S6.7 for data of the other photoacids).

We studied the pH changes of photoacid **3d**, which is more soluble (~8 mM) than the broadly applied alkylsulfonate derivative **2a** (~0.2 mM). Blue light irradiation (λ = 450 nm) of concentrated solutions of **3d** resulted in a drop of the pH value. After the light was removed, the pH recovered to its initial value, making this process fully reversible (Figure 4b). We adjusted the initial pH of the solution ($pH_{initial}$) by addition of minimal amounts of concentrated acid/base and measured the change in pH upon visible light irradiation at different initial pH values. At low pH, the change upon irradiation ($\Delta pH_{h\nu}$) was minimal due to the high concentration of *cis*-MCH and the large proton concentrations needed to induce a change in pH. As the pH increased, the light-induced pH drop increases, reaching a maximum of more than 3 pH units at an initial pH slightly above its pK_a^{dark} value (5.56). At higher initial pH values, the pH drop under irradiation is minimal, due to the very low concentration of MCH and increasing concentration of MC. These observations confirm that increasing the pK_a^{dark} value allows optimized bulk pH changes as the initial pH value is raised.

The maximum change in pH upon irradiation is due to a correlation between the concentration of MCH and the proton concentration needed to result in a change in pH. As indicated above, the significant reduction of the achievable $\Delta pH_{h\nu}$ at higher pH can be partially explained by the very low MCH concentration and the high concentration of hydroxide ions. At very high pH values (pH ≈ 9), blue light irradiation appeared to result in hydrolytic degradation, which is known to occur for merocyanines.[31,33,41b]

Another crucial aspect at high pH is the increasing relative concentration of MC. Previous transient absorption studies[35] of **2a** indicated excitation of MCH to be the predominant pathway to SP formation, with the MC form having a negligible quantum yield (<1%) for photoisomerization to SP. Alkylsulfonate[35,39] and alkylammonium merocyanine[39,43] derivatives have been studied previously at the picosecond timescale to elucidate the isomerization mechanism. It was reported that excitation of **2a**-MCH led to the *trans*-to-*cis* isomerization and deprotonation on a picosecond timescale.[35] Depending on the orientation of the phenolic moiety in the *cis*-MC form, a small proportion was proposed to undergo prompt ring-closure to the SP form (within picoseconds).[35] A longer-lived species was identified as the *cis*-MC form, which needs to rotate around the single bond to undergo ring-closure accounting for the longer lifetime (≫3.5 ns).[35]

We measured the transient absorption of photoacids **2a−c**, **3a−d** from 1 ns to 100 μs at different pH values to observe the decay of this species and calculate the quantum yields of MCH/MC for the SP formation. Representative data of photoacid **3a** are shown in Figure 5. We used aqueous solutions of samples at pH values where the MCH form dominates and pumped at 355 nm to target the MCH absorption band. The decay of the excited-state species (Figure 5a, red) was observed, resulting in a spectrum containing only the persistent ground-state bleach (Figure 5a, blue).

The respective kinetic traces are shown in Figure 5b. The excited-state species with a positive change in optical density (ΔOD) at 520−570 nm decays completely over 100 ns, which we propose to be *cis*-MC, in line with previous assignments.[35]

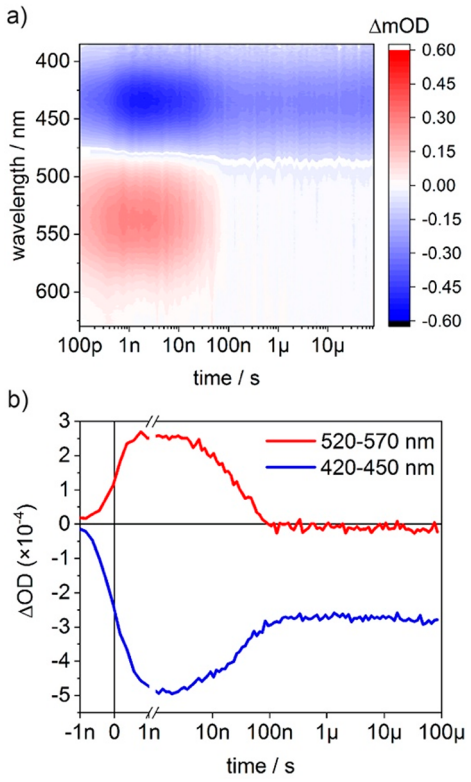

Figure 5. (a) Evolution of the transient absorption spectrum of photoacid **3a** following excitation at 355 nm. Experimental conditions: [**3a**] = 16.7 μM, [phosphate buffer] = 20 mM, pH ≈ 3, T = 25 °C. (b) Respective kinetic traces averaged over a range of selected wavelengths characteristic for the long-lived excited-state species (red) and the ground-state bleach (blue).

This long-lived excited-state species of photoacids **2a−c**, **3a−d** had lifetimes of 30−550 ns, confirming previous estimates for **2a** (≫3.5 ns).[35] The ground-state bleach at 420−450 nm persists to at least 100 μs and corresponds to the maximum absorbance of MCH. The persistent ground-state bleach indicated the concentration of MCH assumed to form SP and was used to calculate the quantum yields of SP formation for photoacids **2a−c**, **3a−d**. Quantum yields for the isomerization of MCH to SP ranged from 3% for **3b** and **3d** to 16% for **2c**. The quantum yield for **2a** was 11%, previously estimated as 37% by UV−vis absorbance,[30,31,42] albeit with excitation at longer wavelengths.

Similar transient absorption measurements at high pH were used to determine the quantum yields of isomerization by MC. For all compounds, these quantum yields were <1% and within error of zero (Supporting Information S7.3, S8). This confirms that the predominant pathway for photoisomerization is from the MCH form. In addition, our pH switching experiments suggest that the isomerization quantum yield of MCH is not a limiting factor to generate bulk pH changes.

With these data in hand, we developed a model to predict the expected pH changes upon irradiation on the basis of the initial pH value. The solubility, pK_a^{dark}, and $pK_a^{h\nu}$ values of the photoacids allow us to predict the pH change upon irradiation at any given initial pH value for any merocyanine with this equilibrium system. Our model assumes the protons contributing to the pH drop solely originate from MCH as well as a complete bleach of MCH upon irradiation (detailed considerations in Supporting Information S11.2).

https://doi.org/10.1021/jacs.1c08810
J. Am. Chem. Soc. 2021, 143, 20758−20768

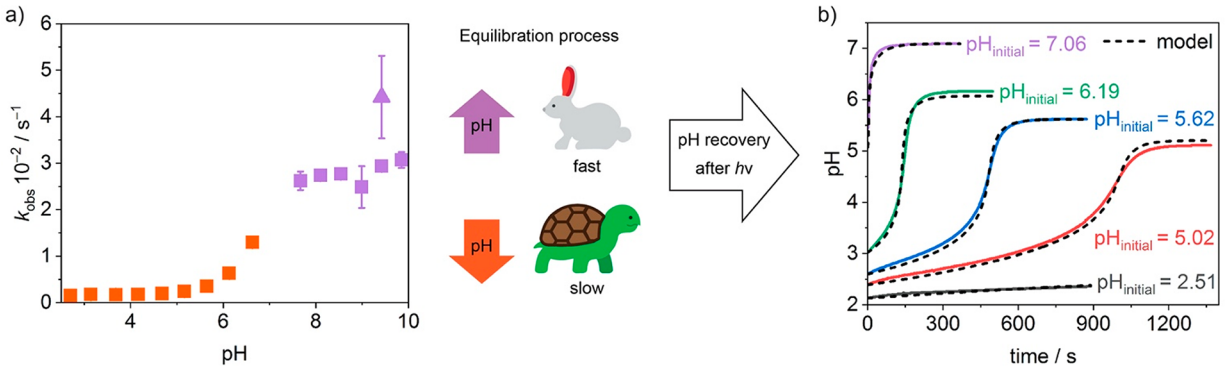

Figure 6. (a) Observed rate constants k_{obs} over the pH range of photoacid **3d** for the thermal equilibration of MC ⇌ SP. Samples at different pH values were measured in 20 mM phosphate buffer to ensure the pH was constant during the isomerization. Rate constants were obtained from a first-order exponential fit to the change in the characteristic absorbance peak (orange, MCH; purple, MC) over time after the equilibrium was perturbed (boxes, change in pH; triangle, after 265 nm light irradiation; see Supporting Information S6.3, S6.6). (b) The pH recovery in the dark of a concentrated solution of **3d** after blue light irradiation (λ = 450 nm); initial pH values before irradiation are indicated, and the respective prediction of the model is shown as dashed lines.

For photoacid **3d**, the model predicts a steady increase of $\Delta pH_{h\nu}$ as the pH value increases (Figure 4c) with a maximum $\Delta pH_{h\nu}$ of ∼3.5 reached at an initial pH value of ∼7−8 (c = 8 mM), followed by a drastic decrease at higher pH. The model matches the experimental data with reasonable accuracy up to an initial pH value of ∼6−7. The model diverges from the experimental data above pH 7 where larger $\Delta pH_{h\nu}$ values were predicted at pH values with a very low MCH concentration ([MCH] ≈ 0). This deviation is likely the result of incomplete beaching under these conditions due to the low isomerization quantum yield of MC and faster thermal processes at high pH values. A less concentrated sample (c ≈ 0.9 mM) also showed this behavior and highlighted the concentration dependence of the resulting pH change. Increasing the concentration of **3d** by one order of magnitude increases the pH drop by one pH unit.

Bulk pH switching experiments were also performed with photoacid **3c** (Supporting Information S10), which confirmed the general trend of increasing $\Delta pH_{h\nu}$ with increasing initial pH values and a drastic decrease of $\Delta pH_{h\nu}$ at higher pH values (∼6). Despite the higher solubility of **3c** (up to ∼20 mM), a maximum $\Delta pH_{h\nu}$ of only ∼2.7 units was observed experimentally. The model predicted a larger $\Delta pH_{h\nu}$ (∼3.8) than we found experimentally with a similar discrepancy in shape as for photoacid **3d**. Some of the divergence of the model can be attributed to concentration effects due to the high solubility of **3c**, as aggregation is known to occur for other merocyanines.[44] We confirmed the concentration-dependence of **3c** above 1 mM by NMR spectroscopy, surprisingly finding that the SP form aggregates at high concentrations (see Supporting Information S5). At lower concentrations of **3c** (c ≈ 0.8 mM), the experimental data is in similar agreement to the pH drop model as for **3d** (Supporting Information S11.4), consistent with negligible aggregation below 1 mM.

For application of these merocyanine photoacids, the timescale of switching is also of the highest importance. Photoacids **2a−c**, **3a−d** studied here rapidly reached photostationary states, typically within 20−30 s at concentrations for UV−visible absorption and for saturated solutions. Therefore, we propose the time-limiting factor for pH switching to be the recovery of pH in the dark after irradiation (Figure 6b), which is nonlinear over time. This is caused by the evolving rate constant k_{obs} of the SP−MC equilibrium as the pH recovers over time in the dark. We developed a model to describe the pH recovery over time considering the pH-dependent parameters k_{obs}, the concentrations of MCH, MC, and SP, the extent of the photoisomerization to SP ("bleaching"), as well as the equilibrium with water defined by K_w (details in Supporting Information S12). We assumed the protonation events are sufficiently fast that they could be modeled as thermodynamic equilibria defined by K_a, $K_a^{h\nu}$, and K_w, and we incorporated the K_c equilibrium as kinetic steps. Parameters were constrained within experimental errors with the largest error stemming from the sensitivity of the kinetic parameters to temperature. As our experimental setup could only limit temperature fluctuations <1 °C at best, the error margin for k_c and k_o was slightly increased to account for this. We did not include a thermal *cis*-MCH to MCH process as such an isomerization has been proposed to be very slow as compared to equilibration between *cis*-MCH and SP, albeit for a different spiropyran derivative.[36] Further details are provided in Supporting Information S12, along with the Python code used in the modeling.

The model reproduces the experimental lineshape, timescale, and pH recovery values well, with some minor deviations in lineshape and the final equilibrium positions. Slight temperature fluctuations during the pH recovery result in a variation of the temperature-dependent rate constants k_o and k_c, which are modeled as constants. This sensitivity to temperature could account for the small deviations between the model and the experimental data.

Very small changes in concentrations, the many interlinked equilibrium processes, and sensitivity to temperature changes make these systems highly susceptible to small changes and challenging to model. Nonetheless, we can see that, depending on the initial pH, the measured recovery of the same photoacid (**3d**) varied by almost one order of magnitude ($pH_{initial}$ 7.06, apparent $t_{1/2}$ ≈ 1.4 min; $pH_{initial}$ 5.02, apparent $t_{1/2}$ ≈ 10 min) over the same pH range, as estimated from the data in Figure 6b. The nonlinear behavior of the system and pH-tunability could give rise to interesting applications. Implementation of switching cycles, which do not allow full recovery, could enable fast cycling, for example, between pH 5 and 6, by timing the irradiation and recovery time of the system. Modifying the speed of pH recovery could also open new opportunities, for example, in gel research, where control over the pH tunes the properties of the gel.

https://doi.org/10.1021/jacs.1c08810
J. Am. Chem. Soc. 2021, 143, 20758−20768

We demonstrated the reversibility of visible light-induced pH switching of photoacid **3d** at reasonable timescales (2−3 min per cycle at ambient temperature). Photoacid **3d** has the highest reported pK_a^{dark} value (5.56) of the alkylammonium merocyanine derivatives, and combined with its good solubility we were able to switch the pH of a solution by ∼3.2 units from pH 6.5 to pH 3.3 over 16 cycles without showing significant decomposition (Figure 7, loss of ΔpH = 0.1). By comparison, photoacid **2a** and its analogue with a butyl sulfonate chain (**5**) have exhibited pH switching of ∼2 and 2.5 units, respectively.[16a,31] A very recent report of a related methoxy derivative increased this pH switching to 3 units.[32]

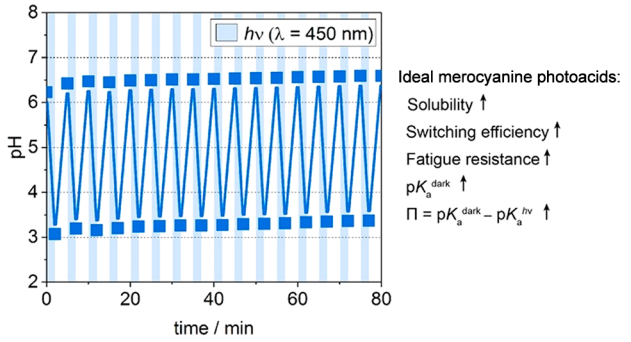

Figure 7. Visible light-induced (λ = 450 nm, indicated by blue boxes) pH switching of a concentrated solution of photoacid **3d** (∼8 mM) by ∼3.2 units over 16 cycles (left). Highlighting key parameters of merocyanine photoacids to optimize light-induced pH switching (right).

CONCLUSIONS

We have determined the key parameters that underpin the photoacidity and thermal recovery processes of merocyanines **2b−d** and **3a−d**. The pH switching range is dictated by the thermodynamic parameters pK_a^{dark} and $pK_a^{h\nu}$, as well as the solubility, while the speed of the pH recovery in the dark is controlled by kinetic parameters (k_o, k_c). The photoacidity (Π) appears to be relatively constant regardless of the substitution pattern. These key parameters allow the pH switching behavior of merocyanine photoacids to be predicted. Comparison with the literature provides an understanding of how electronic effects influence these parameters, providing clear guidelines for future designs. Specific and reversible pH changes can be accessed by choosing a suitable photoacid, making merocyanine photoacids an incredibly useful tool for generating custom pH changes with visible light.

We identified that increasing pK_a^{dark} values and operating the merocyanine photoacids at higher pH values maximized the achievable light-induced pH changes. The upper pH operating range is limited by the pK_a^{dark} value and the autoionization of water. The solubility also plays a crucial role in changing bulk pH values with alkylammonium-functionalized merocyanines being more soluble than alkylsulfonate derivatives, with higher concentrations resulting in larger pH changes.

The quantitative model we developed allows the prediction of light-induced pH changes based on the concentration, pK_a^{dark}, and $pK_a^{h\nu}$ values and can be applied to many merocyanine photoacids (see Supporting Information S11,S12). We have also developed a kinetic model to describe the rate of pH recovery in the dark after visible light irradiation, which is in agreement with our experimental data and may also prove generally applicable to merocyanine photoacids. Finally, we were able to increase the light-induced pH change of merocyanine photoacids to ∼3.2 units (pH 6.5 to pH 3.3) using photoacid **3d** with high reversibility.

Ultimately, the pH changes that can be obtained will depend on the buffering capacity of the system. That is, the pH changes we demonstrate are the maximum for these compounds as the solution does not contain other ions (other than KCl) that can buffer the changes in pH. The ability to tune the magnitude and timescales of pH switching offers exciting new possibilities in any research area that applies pH to control chemical or biological processes, including using photoswitches to drive systems away from equilibrium.[45]

ASSOCIATED CONTENT

Supporting Information

The Supporting Information is available free of charge at https://pubs.acs.org/doi/10.1021/jacs.1c08810.

Synthetic procedures, spectroscopic data, and all photoswitching and fitted data (PDF)

Photoacid switching code, included as a Jupyter notebook (ipynb); this format allows a readable combination of code and results and is a standard for data exploration (ZIP)

AUTHOR INFORMATION

Corresponding Author

Jonathon E. Beves − *School of Chemistry, UNSW Sydney, Sydney, New South Wales 2052, Australia;* orcid.org/0000-0002-5997-6580; Email: j.beves@unsw.edu.au

Authors

Laura Wimberger − *School of Chemistry, UNSW Sydney, Sydney, New South Wales 2052, Australia*

Shyamal K. K. Prasad − *School of Chemistry, UNSW Sydney, Sydney, New South Wales 2052, Australia*

Martin D. Peeks − *School of Chemistry, UNSW Sydney, Sydney, New South Wales 2052, Australia;* orcid.org/0000-0002-9057-9444

Joakim Andréasson − *Department of Chemistry and Chemical Engineering, Chalmers University of Technology, Göteborg 412 96, Sweden*

Timothy W. Schmidt − *School of Chemistry, UNSW Sydney, Sydney, New South Wales 2052, Australia;* orcid.org/0000-0001-6691-1438

Complete contact information is available at: https://pubs.acs.org/10.1021/jacs.1c08810

Notes

The authors declare no competing financial interest.

ACKNOWLEDGMENTS

This work was supported by the Australian Research Council (J.E.B., FT170100094; T.W.S., S.K.K.P., and J.E.B., Centre of Excellence in Exciton Science CE170100026). We acknowledge the Mark Wainwright Analytical Centre at UNSW Sydney for access to the NMR facility.

REFERENCES

(1) (a) Hull, J. F.; Himeda, Y.; Wang, W.-H.; Hashiguchi, B.; Periana, R.; Szalda, D. J.; Muckerman, J. T.; Fujita, E. Reversible hydrogen storage using CO_2 and a proton-switchable iridium catalyst in aqueous

media under mild temperatures and pressures. *Nat. Chem.* **2012**, *4*, 383−388. (b) Geri, J. B.; Szymczak, N. K. A Proton-Switchable Bifunctional Ruthenium Complex That Catalyzes Nitrile Hydroboration. *J. Am. Chem. Soc.* **2015**, *137*, 12808−12814. (c) Semwal, S.; Choudhury, J. Molecular Coordination-Switch in a New Role: Controlling Highly Selective Catalytic Hydrogenation with Switchability Function. *ACS Catal.* **2016**, *6*, 2424−2428. (d) Blyth, M. T.; Coote, M. L. A pH-Switchable Electrostatic Catalyst for the Diels−Alder Reaction: Progress toward Synthetically Viable Electrostatic Catalysis. *J. Org. Chem.* **2019**, *84*, 1517−1522. (e) Arlegui, A.; Torres, P.; Cuesta, V.; Crusats, J.; Moyano, A. A pH-Switchable Aqueous Organocatalysis with Amphiphilic Secondary Amine−Porphyrin Hybrids. *Eur. J. Org. Chem.* **2020**, *2020*, 4399−4407.

(2) (a) Branda, N.; Grotzfeld, R. M.; Valdes, C.; Rebek, J., Jr. Control of Self-Assembly and Reversible Encapsulation of Xenon in a Self-Assembling Dimer by Acid-Base Chemistry. *J. Am. Chem. Soc.* **1995**, *117*, 85−88. (b) Ibukuro, F.; Kusukawa, T.; Fujita, M. A Thermally Switchable Molecular Lock. Guest-Templated Synthesis of a Kinetically Stable Nanosized Cage. *J. Am. Chem. Soc.* **1998**, *120*, 8561−8562. (c) Grote, Z.; Scopelliti, R.; Severin, K. pH-Triggered Assembly of Organometallic Receptors for Lithium Ions. *J. Am. Chem. Soc.* **2004**, *126*, 16959−16972. (d) Gottschalk, T.; Jaun, B.; Diederich, F. Container Molecules with Portals: Reversibly Switchable Cycloalkane Complexation. *Angew. Chem., Int. Ed.* **2007**, *46*, 260−264. (e) Mal, P.; Schultz, D.; Beyeh, K.; Rissanen, K.; Nitschke, J. R. An Unlockable−Relockable Iron Cage by Subcomponent Self-Assembly. *Angew. Chem., Int. Ed.* **2008**, *47*, 8297−8301. (f) Carvalho, C. P.; Uzunova, V. D.; Da Silva, J. P.; Nau, W. M.; Pischel, U. A photoinduced pH jump applied to drug release from cucurbit[7]uril. *Chem. Commun.* **2011**, *47*, 8793−8795. (g) Isaacs, L. Stimuli Responsive Systems Constructed Using Cucurbit[n]uril-Type Molecular Containers. *Acc. Chem. Res.* **2014**, *47*, 2052−2062. (h) Altmann, P. J.; Pöthig, A. A pH-Dependent, Mechanically Interlocked Switch: Organometallic [2]Rotaxane vs. Organic [3]Rotaxane. *Angew. Chem., Int. Ed.* **2017**, *56*, 15733−15736.

(3) (a) Bruns, C. J.; Stoddart, J. F. Rotaxane-Based Molecular Muscles. *Acc. Chem. Res.* **2014**, *47*, 2186−2199. (b) Zhou, H. Y.; Han, Y.; Chen, C. F. pH-Controlled motions in mechanically interlocked molecules. *Mater. Chem. Phys.* **2020**, *4*, 12−28. (c) Rizzuto, F. J.; Platnich, C. M.; Luo, X.; Shen, Y.; Dore, M. D.; Lachance-Brais, C.; Guarne, A.; Cosa, G.; Sleiman, H. F. A dissipative pathway for the structural evolution of DNA fibres. *Nat. Chem.* **2021**, *13*, 843.

(4) (a) Bissell, R. A.; Cordova, E.; Kaifer, A. E.; Stoddart, J. F. A chemically and electrochemically switchable molecular shuttle. *Nature* **1994**, *369*, 133−137. (b) Ashton, P. R.; Ballardini, R.; Balzani, V.; Baxter, I.; Credi, A.; Fyfe, M. C. T.; Gandolfi, M. T.; Gómez-López, M.; Martínez-Díaz, M. V.; Piersanti, A.; Spencer, N.; Stoddart, J. F.; Venturi, M.; White, A. J. P.; Williams, D. J. Acid-Base Controllable Molecular Shuttles. *J. Am. Chem. Soc.* **1998**, *120*, 11932−11942. (c) Crowley, J. D.; Leigh, D. A.; Lusby, P. J.; McBurney, R. T.; Perret-Aebi, L.-E.; Petzold, C.; Slawin, A. M. Z.; Symes, M. D. A Switchable Palladium-Complexed Molecular Shuttle and Its Metastable Positional Isomers. *J. Am. Chem. Soc.* **2007**, *129*, 15085−15090.

(5) Irie, M. Light-induced reversible pH change. *J. Am. Chem. Soc.* **1983**, *105*, 2078−2079.

(6) (a) Pines, E.; Huppert, D.; Agmon, N. Geminate recombination in excited-state proton-transfer reactions: Numerical solution of the Debye−Smoluchowski equation with backreaction and comparison with experimental results. *J. Chem. Phys.* **1988**, *88*, 5620−5630. (b) Spies, C.; Finkler, B.; Acar, N.; Jung, G. Solvatochromism of pyranine-derived photoacids. *Phys. Chem. Chem. Phys.* **2013**, *15*, 19893−19905.

(7) Also reported as 7.8 versus 0.4, see: Pines, E.; Huppert, D. pH jump: a relaxational approach. *J. Phys. Chem.* **1983**, *87*, 4471−4478.

(8) (a) Yucknovsky, A.; Mondal, S.; Burnstine-Townley, A.; Foqara, M.; Amdursky, N. Use of Photoacids and Photobases To Control Dynamic Self-Assembly of Gold Nanoparticles in Aqueous and Nonaqueous Solutions. *Nano Lett.* **2019**, *19*, 3804−3810. (b) Legrand, A.; Liu, L.-H.; Royla, P.; Aoyama, T.; Craig, G. A.; Carné-Sánchez, A.; Urayama, K.; Weigand, J. J.; Lin, C.-H.; Furukawa, S. Spatiotemporal Control of Supramolecular Polymerization and Gelation of Metal−Organic Polyhedra. *J. Am. Chem. Soc.* **2021**, *143*, 3562−3570.

(9) Significant pK_a changes have been reported for azobenzene-type switches, see: (a) Beharry, A. A.; Sadovski, O.; Woolley, G. A. Azobenzene Photoswitching without Ultraviolet Light. *J. Am. Chem. Soc.* **2011**, *133*, 19684−19687. (b) Emond, M.; Sun, J.; Grégoire, J.; Maurin, S.; Tribet, C.; Jullien, L. Photoinduced pH drops in water. *Phys. Chem. Chem. Phys.* **2011**, *13*, 6493−6499. (c) Weston, C. E.; Richardson, R. D.; Fuchter, M. J. Photoswitchable basicity through the use of azoheteroarenes. *Chem. Commun.* **2016**, *52*, 4521−4524. (d) Kennedy, A. D. W.; Sandler, I.; Andréasson, J.; Ho, J.; Beves, J. E. Visible-Light Photoswitching by Azobenzazoles. *Chem. - Eur. J.* **2020**, *26*, 1103−1110. (e) Ludwanowski, S.; Ari, M.; Parison, K.; Kalthoum, S.; Straub, P.; Pompe, N.; Weber, S.; Walter, M.; Walther, A. pH Tuning of Water-Soluble Arylazopyrazole Photoswitches. *Chem. - Eur. J.* **2020**, *26*, 13203−13212. For an example of pK_a changes of an azobenzene-type switch with pK_a, *E* 7.2, *Z* 5.7, see: (f) Samanta, S.; Babalhavaeji, A.; Dong, M.-X.; Woolley, G. A. Photoswitching of *ortho*-Substituted Azonium Ions by Red Light in Whole Blood. *Angew. Chem., Int. Ed.* **2013**, *52*, 14127−14130. For an example of pK_a changes with an azobenzene-type switch of pK_a, *E* 4.7, *Z* 6.0, see part (c). For examples of pK_a switching using diarylethenes, see: (g) Kawai, S. H.; Gilat, S. L.; Lehn, J.-M. Photochemical pK_a-Modulation and Gated Photochromic Properties of a Novel Diarylethene Switch. *Eur. J. Org. Chem.* **1999**, 2359−2366. (h) Massaad, J.; Micheau, J.-C.; Coudret, C.; Sanchez, R.; Guirado, G.; Delbaere, S. Gated Photochromism and Acidity Photomodulation of a Diacid Dithienylethene Dye. *Chem.- Eur. J.* **2012**, *18*, 6568−6575. For an example of a diarylethenewith pK_a, open 10.2, closed 9.0, see: (i) Odo, Y.; Matsuda, K.; Irie, M. pK_a Switching Induced by the Change in the π-Conjugated System Based on Photochromism. *Chem.- Eur. J.* **2006**, *12*, 4283−4288. For a diarylethene with pK_a, open 4.0, closed 6.8, see: (j) Gurke, J.; Budzák, Š.; Schmidt, B. M.; Jacquemin, D.; Hecht, S. Efficient Light-Induced pK_a-Modulation Coupled to Base-Catalyzed Photochromism. *Angew. Chem., Int. Ed.* **2018**, *57*, 4797−4801. For pK_a switching with hemithioindigos with pK_a, *trans* 7.2, *cis* 5.0, see: (k) Koeppe, B.; Rühl, S.; Römpp, F. Towards More Effective, Reversible pH Control by Visible Light Alone: A Thioindigo Photoswitch Undergoing a Strong pK_a Modulation by Isomer-Specific Hydrogen Bonding. *ChemPhotoChem.* **2019**, *3*, 71−74. For pK_a switching using nitrile-rich photoswitches with pK_a, closed 3.9, open 6.6, see: (l) Belikov, M. Y.; Ievlev, M. Y.; Bardasov, I. N. A novel water-soluble multicolor halo- and photochromic switching system based on a nitrile-rich acceptor. *New J. Chem.* **2021**, *45*, 10287−10295.

(10) (a) Klajn, R. Spiropyran-based dynamic materials. *Chem. Soc. Rev.* **2014**, *43*, 148−184. (b) Kortekaas, L.; Browne, W. R. The evolution of spiropyran: fundamentals and progress of an extraordinarily versatile photochrome. *Chem. Soc. Rev.* **2019**, *48*, 3406−3424.

(11) (a) Raymo, F. M.; Giordani, S. Signal Processing at the Molecular Level. *J. Am. Chem. Soc.* **2001**, *123*, 4651−4652. (b) Raymo, F. M.; Giordani, S.; White, A. J. P.; Williams, D. J. Digital Processing with a Three-State Molecular Switch. *J. Org. Chem.* **2003**, *68*, 4158−4169.

(12) Silvi, S.; Arduini, A.; Pochini, A.; Secchi, A.; Tomasulo, M.; Raymo, F. M.; Baroncini, M.; Credi, A. A Simple Molecular Machine Operated by Photoinduced Proton Transfer. *J. Am. Chem. Soc.* **2007**, *129*, 13378−13379.

(13) (a) Silvi, S.; Constable, E. C.; Housecroft, C. E.; Beves, J. E.; Dunphy, E. L.; Tomasulo, M.; Raymo, F. M.; Credi, A. Photochemical switching of luminescence and singlet oxygen generation by chemical signal communication. *Chem. Commun.* **2009**, 1484−1486. (b) Silvi, S.; Constable, E. C.; Housecroft, C. E.; Beves, J. E.; Dunphy, E. L.; Tomasulo, M.; Raymo, F. M.; Credi, A. All-Optical Integrated Logic Operations Based on Chemical Communication between Molecular Switches. *Chem. - Eur. J.* **2009**, *15*, 178−185.

(14) Raymo, F. M.; Giordani, S. Signal Communication between Molecular Switches. *Org. Lett.* **2001**, *3*, 3475−3478.

(15) Miskolczy, Z.; Biczók, L. Photochromism in Cucurbit[8]uril Cavity: Inhibition of Hydrolysis and Modification of the Rate of

https://doi.org/10.1021/jacs.1c08810
J. Am. Chem. Soc. 2021, 143, 20758−20768

Merocyanine−Spiropyran Transformations. *J. Phys. Chem. B* **2011**, *115*, 12577−12583.
(16) (a) Shi, Z.; Peng, P.; Strohecker, D.; Liao, Y. Long-Lived Photoacid Based upon a Photochromic Reaction. *J. Am. Chem. Soc.* **2011**, *133*, 14699−14703. (b) Liao, Y. Design and Applications of Metastable-State Photoacids. *Acc. Chem. Res.* **2017**, *50*, 1956−1964.
(17) The analogue that includes the *para*-NO_2 group has a pK_a in the dark of 6.36, around 1.5 units higher than that of **2a**, see ref 16a.
(18) (a) Shi, Q.; Chen, C. F. Switchable Complexation between (O-Methyl)6−2,6-helic[6]arene and Protonated Pyridinium Salts Controlled by Acid/Base and Photoacid. *Org. Lett.* **2017**, *19*, 3175−3178. (b) Jansze, S. M.; Cecot, G.; Severin, K. Reversible disassembly of metallasupramolecular structures mediated by a metastable-state photoacid. *Chem. Sci.* **2018**, *9*, 4253−4257. (c) Kothapalli, S. S. K.; Kannekanti, V. K.; Ye, Z. C.; Yang, Z. Y.; Chen, L. X.; Cai, Y. M.; Zhu, B. C.; Feng, W.; Yuan, L. H. Light-controlled switchable complexation by a non-photoresponsive hydrogen-bonded amide macrocycle. *Org. Chem. Front.* **2020**, *7*, 846−855. (d) Li, R.-J.; Pezzato, C.; Berton, C.; Severin, K. Light-induced assembly and disassembly of polymers with PdnL2n-type network junctions. *Chem. Sci.* **2021**, *12*, 4981−4984.
(19) (a) Guo, J.; Zhang, H. Y.; Zhou, Y.; Liu, Y. Light-controlled reversible self-assembly of nanorodsuprastructures. *Chem. Commun.* **2017**, *53*, 6089−6092. (b) Cissé, N.; Kudernac, T. Light-Fuelled Self-Assembly of Cyclic Peptides into Supramolecular Tubules. *ChemSystemsChem.* **2020**, *2*, No. e2000012. (c) Chen, X.-M.; Hou, X.-F.; Bisoyi, H. K.; Feng, W.-J.; Cao, Q.; Huang, S.; Yang, H.; Chen, D.; Li, Q. Light-fueled transient supramolecular assemblies in water as fluorescence modulators. *Nat. Commun.* **2021**, *12*, 4993.
(20) Ryssy, J.; Natarajan, A. K.; Wang, J.; Lehtonen, A. J.; Nguyen, M. K.; Klajn, R.; Kuzyk, A. Light-Responsive Dynamic DNA-Origami-Based Plasmonic Assemblies. *Angew. Chem., Int. Ed.* **2021**, *60*, 5859−5863.
(21) For an example using the *N*-Me spiropyran deriviative instead of **2a**, see: Kundu, P. K.; Samanta, D.; Leizrowice, R.; Margulis, B.; Zhao, H.; Börner, M.; Udayabhaskararao, T.; Manna, D.; Klajn, R. Light-controlled self-assembly of non-photoresponsive nanoparticles. *Nat. Chem.* **2015**, *7*, 646−652.
(22) (a) Moreno, S.; Sharan, P.; Engelke, J.; Gumz, H.; Boye, S.; Oertel, U.; Wang, P.; Banerjee, S.; Klajn, R.; Voit, B.; Lederer, A.; Appelhans, D. Light-Driven Proton Transfer for Cyclic and Temporal Switching of Enzymatic Nanoreactors. *Small* **2020**, *16*, 2002135. (b) Qu, P.; Kuepfert, M.; Hashmi, M.; Weck, M. Compartmentalization and Photoregulating Pathways for Incompatible Tandem Catalysis. *J. Am. Chem. Soc.* **2021**, *143*, 4705−4713.
(23) For an example using the *para*-NO_2 spiropyran derviative attached to a polymer via a linker from the amine, see: Li, C.; Iscen, A.; Sai, H.; Sato, K.; Sather, N. A.; Chin, S. M.; Álvarez, Z.; Palmer, L. C.; Schatz, G. C.; Stupp, S. I. Supramolecular−covalent hybrid polymers for light-activated mechanical actuation. *Nat. Mater.* **2020**, *19*, 900−909.
(24) (a) Maity, C.; Hendriksen, W. E.; van Esch, J. H.; Eelkema, R. Spatial Structuring of a Supramolecular Hydrogel by using a Visible-Light Triggered Catalyst. *Angew. Chem., Int. Ed.* **2015**, *54*, 998−1001. (b) Li, X.; Fei, J.; Xu, Y.; Li, D.; Yuan, T.; Li, G.; Wang, C.; Li, J. A Photoinduced Reversible Phase Transition in a Dipeptide Supramolecular Assembly. *Angew. Chem., Int. Ed.* **2018**, *57*, 1903−1907.
(25) Zhang, T.; Sheng, L.; Liu, J.; Ju, L.; Li, J.; Du, Z.; Zhang, W.; Li, M.; Zhang, S. X.-A. Photoinduced Proton Transfer between Photoacid and pH-Sensitive Dyes: Influence Factors and Application for Visible-Light-Responsive Rewritable Paper. *Adv. Funct. Mater.* **2018**, *28*, 1705532.
(26) Fu, C.; Xu, J.; Boyer, C. Photoacid-mediated ring opening polymerization driven by visible light. *Chem. Commun.* **2016**, *52*, 7126−7129.
(27) Tatum, L. A.; Foy, J. T.; Aprahamian, I. Waste management of chemically activated switches: using a photoacid to eliminate accumulation of side products. *J. Am. Chem. Soc.* **2014**, *136*, 17438−17441.
(28) Xu, Y.; Fei, J.; Li, G.; Yuan, T.; Li, Y.; Wang, C.; Li, X.; Li, J. Enhanced Photophosphorylation of a Chloroplast-Entrapping Long-Lived Photoacid. *Angew. Chem., Int. Ed.* **2017**, *56*, 12903−12907.
(29) Shi, Q.; Meng, Z.; Xiang, J.-F.; Chen, C.-F. Efficient control of movement in non-photoresponsive molecular machines by a photo-induced proton-transfer strategy. *Chem. Commun.* **2018**, *54*, 3536−3539.
(30) Vallet, J.; Micheau, J. C.; Coudret, C. Switching a pH indicator by a reversible photoacid: A quantitative analysis of a new two-component photochromic system. *Dyes Pigm.* **2016**, *125*, 179−184.
(31) Berton, C.; Busiello, D. M.; Zamuner, S.; Solari, E.; Scopelliti, R.; Fadaei-Tirani, F.; Severin, K.; Pezzato, C. Thermodynamics and kinetics of protonated merocyanine photoacids in water. *Chem. Sci.* **2020**, *11*, 8457−8468.
(32) Berton, C.; Busiello, D. M.; Zamuner, S.; Scopelliti, R.; Fadaei-Tirani, F.; Severin, K.; Pezzato, C. Light-switchable buffers. *Angew. Chem., Int. Ed.* **2021**, *60*, 21737−21740.
(33) (a) Hammarson, M.; Nilsson, J. R.; Li, S.; Beke-Somfai, T.; Andréasson, J. Characterization of the Thermal and Photoinduced Reactions of Photochromic Spiropyrans in Aqueous Solution. *J. Phys. Chem. B* **2013**, *117*, 13561−13571. (b) Abeyrathna, N.; Liao, Y. Stability of merocyanine-type photoacids in aqueous solutions. *J. Phys. Org. Chem.* **2017**, *30*, No. e3664.
(34) Fleming, C. L.; Li, S.; Grøtli, M.; Andréasson, J. Shining New Light on the Spiropyran Photoswitch: A Photocage Decides between cis−trans or Spiro-Merocyanine Isomerization. *J. Am. Chem. Soc.* **2018**, *140*, 14069−14072.
(35) Aldaz, C. R.; Wiley, T. E.; Miller, N. A.; Abeyrathna, N.; Liao, Y.; Zimmerman, P. M.; Sension, R. J. Experimental and Theoretical Characterization of Ultrafast Water-Soluble Photochromic Photoacids. *J. Phys. Chem. B* **2021**, *125*, 4120−4131.
(36) Kortekaas, L.; Chen, J.; Jacquemin, D.; Browne, W. R. Proton-Stabilized Photochemically Reversible *E*/*Z* Isomerization of Spiropyrans. *J. Phys. Chem. B* **2018**, *122*, 6423−6430.
(37) Liu, J.; Tang, W.; Sheng, L.; Du, Z.; Zhang, T.; Su, X.; Zhang, S. X.-A. Effects of Substituents on Metastable-State Photoacids: Design, Synthesis, and Evaluation of their Photochemical Properties. *Chem. - Asian J.* **2019**, *14*, 438−445.
(38) Wojtyk, J. T. C.; Buncel, E.; Kazmaier, P. M. Effects of metal ion complexation on the spiropyran−merocyanine interconversion: development of a thermally stable photo-switch. *Chem. Commun.* **1998**, 1703−1704.
(39) Kaiser, C.; Halbritter, T.; Heckel, A.; Wachtveitl, J. Proton-Transfer Dynamics of PhotoacidicMerocyanines in Aqueous Solution. *Chem. - Eur. J.* **2021**, *27*, 9160−9173.
(40) For a detailed discussion of the identification of *cis*-MCH, see ref 36.
(41) (a) Satoh, T.; Sumaru, K.; Takagi, T.; Takai, K.; Kanamori, T. Isomerization of spirobenzopyrans bearing electron-donating and electron-withdrawing groups in acidic aqueous solutions. *Phys. Chem. Chem. Phys.* **2011**, *13*, 7322−7329. (b) Moldenhauer, D.; Gröhn, F. Water-Soluble Spiropyrans with Inverse Photochromism and Their Photoresponsive Electrostatic Self-Assembly. *Chem. - Eur. J.* **2017**, *23*, 3966−3978.
(42) Johns, V. K.; Wang, Z.; Li, X.; Liao, Y. Physicochemical Study of a Metastable-State Photoacid. *J. Phys. Chem. A* **2013**, *117*, 13101−13104.
(43) Kaiser, C.; Halbritter, T.; Heckel, A.; Wachtveitl, J. Thermal, Photochromic and Dynamic Properties of Water-Soluble Spiropyrans. *ChemistrySelect* **2017**, *2*, 4111−4123.
(44) Zhang, Y.; Ng, M.; Hong, E. Y.-H.; Chan, A. K.-W.; Wu, N. M.-W.; Chan, M. H.-Y.; Wu, L.; Yam, V. W.-W. Synthesis and photoswitchableamphiphilicity and self-assembly properties of photochromic spiropyran derivatives. *J. Mater. Chem. C* **2020**, *8*, 13676−13685.
(45) (a) Kathan, M.; Hecht, S. Photoswitchable molecules as key ingredients to drive systems away from the global thermodynamic minimum. *Chem. Soc. Rev.* **2017**, *46*, 5536−5550. (b) Andréasson, J.; Pischel, U. Light-stimulated molecular and supramolecular systems for

https://doi.org/10.1021/jacs.1c08810
J. Am. Chem. Soc. 2021, 143, 20758−20768

information processing and beyond. *Coord. Chem. Rev.* **2021**, *429*, 213695.

https://doi.org/10.1021/jacs.1c08810
J. Am. Chem. Soc. 2021, 143, 20758−20768